$AM_3(P_2O_7)_2$ (A = Alkaline-Earth Metals; M = Fe, Co, Ni): Diphosphates Containing Infinite Chains of Edge-Sharing MO_6 Octahedra

Kwang-Hwa Lii*

Institute of Chemistry, Academia Sinica, Nankang, Taipei, Taiwan, ROC

Pei-Fen Shih and Teng-Ming Chen

Department of Applied Chemistry, National Chiao Tung University, Hsinchu, Taiwan, ROC

Received January 14, 1993®

Diphosphates of the stoichiometry $AM_3(P_2O_7)_2$ (A = alkaline-earth metals; M = Fe, Co, Ni) have been synthesized and structurally characterized by single-crystal X-ray diffraction. Crystal data: $CaNi_3(P_2O_7)_2$, monoclinic, $P2_1/c$, a = 7.330(3) Å, b = 7.589(3) Å, c = 9.400(3) Å, β = 111.90(3)°, V = 485.1(3) Å^3, Z = 2, and R = 0.026; $CaCo_3(P_2O_7)_2$, as above except a = 7.394(1) Å, b = 7.6266(9) Å, c = 9.444(2) Å, β = 111.73(2)°, V = 494.7(1) Å^3, and R = 0.035; $SrFe_3(P_2O_7)_2$, as above except a = 7.553(1) Å, b = 7.7477(8) Å, c = 9.5796(8) Å, β = 112.11(1)°, V = 519.4(1) Å^3, and R = 0.029. The three compounds are isostructural, consisting of zigzag infinite chains of MO_6 octahedra sharing either trans or skew edges. The infinite chains are connected by P_2O_7 groups to form a three-dimensional architecture with channels parallel to the b axis. Alkaline-earth metals are located in sites within the channels. The following isostructural compounds have also been prepared: $AM_3(P_2O_7)_2$ (A = Sr, Ba; M = Ni, Co) and $BaFe_3(P_2O_7)_2$. A magnetic susceptibility study on $SrFe_3(P_2O_7)_2$ indicates that the material is paramagnetic with an effective magnetic moment of 5.07 μ_B per Fe between 300 and 26 K. Below this temperature the magnetic susceptibility increases sharply to a maximum at 6 K and then decreases rapidly. Mossbauer spectra also confirm the presence of Fe(II).

Introduction

Recently we synthesized and structurally characterized several new compounds in the ternary vanadium phosphate system. Compounds such as β-$K_2V_3P_4O_{17}$,[1] β-$LiVOPO_4$,[2] $Ca(VO)_2(PO_4)_2$,[3] $A(VOPO_4)_2 \cdot nH_2O$ (A = Na, K, Rb, Ca, Sr, Pb, Co, Ni; n = 3, 4),[4-6] $Ca_2V(PO_4)(HPO_4)_2 \cdot H_2O$,[7] and $Ca_2V(PO_4)(P_2O_7)$[7] have been synthesized. These phosphates are of interest for their complex tetrahdral–octahedral network structures. Our synthetic approaches were twofold, namely high-temperature solid-state reactions and hydrothermal methods. Hydrothermal synthesis involves the use of aqueous solvents or mineralizers under high temperature and high pressure to dissolve and recrystallize materials that are relatively insoluble under ordinary conditions. Since hydrothermal methods proved to be particularly suitable for crystal growth, we recently extended our research to the synthesis of phosphate crystals of other transition metals from phosphoric acid solutions under hydrothermal conditions. To begin with, we studied iron and nickel systems, as basic and/or hydrated iron phosphate minerals are considered as among the most perplexing substances in the mineral kingdom,[8] and few ternary nickel phosphates are known. Several new compounds in the iron system have been synthesized: $SrFe_3(PO_4)_3(HPO_4)$,[9] $CaFe_2(PO_4)_2(HPO_4)$,[10] and $AFe_5(PO_4)_5(OH) \cdot H_2O$ (A = Ca, Sr).[11] The structures of these phosphates cover discrete FeO_5 trigonal bipyramids, FeO_6 octahedra, and dimers of corner-sharing, edge-sharing, and face-sharing FeO_6 octahedra. We have now prepared a ferrous phosphate, $SrFe_3(P_2O_7)_2$, which consists of zigzag infinite chains of FeO_6 octahedra sharing either trans or skew edges. The compounds $CaM_3(P_2O_7)_2$ (M = Ni, Co) appear as members of a series of isomorphous diphosphates. In the work presented herein, we report the synthesis, single-crystal X-ray structures, magnetic susceptibilities, and Mossbauer spectroscopy of $CaNi_3(P_2O_7)_2$, $CaCO_3(P_2O_7)_2$, and $SrFe_3(P_2O_7)_2$.

Experimental Section

Synthesis. Reagent grade chemicals were used as received. The crystal growth was achieved by heating metal hydroxides or oxides in appropriate proportions in dilute phosphoric acid solution in a quartz glass tube at 500 °C for several days followed by slow cooling. The glass tube was about 50% filled, including the volume of undissolved solid. The glass tube was heated in a pressure vessel in which the pressure inside the tube was balanced by an external pressure to keep the tube intact. The pressure in the quartz tube under the reaction conditions was estimated to be 970 bar according to the pressure–temperature diagram of pure water. It should be noted that the vapor pressure over aqeuous solutions is in general less than that over pure water and the critical point is shifted to higher temperatures. The products were filtered off, washed with water, rinsed with ethanol, and dried at ambient temperature. For example, yellow plate crystals of $CaNi_3(P_2O_7)_2$ were obtained by heating $Ca(OH)_2$ (0.0572 g), $Ni(OH)_2$ (0.2142 g), and H_3PO_4 (2 mL, 3.75 M) (molar ratio Ca:Ni:P = 1:3:~10) in a quartz glass tube at 500 °C for 60 h and then cooling to room temperature over 12 h. Powder X-ray diffraction of the bulk product indicated that a single phase of $CaNi_3(P_2O_7)_2$ was produced. The solid-state reaction of $Ca_3(PO_4)_2$, NiO, and P_2O_5 (molar ratio 1:9:5) in a sealed glass tube, at 900 °C for 2 d, led to a single-phase polycrystalline product. Hydrothermal treatment of 0.0695 g of $Ca(OH)_2$ (or 0.1104 g of $Sr(OH)_2 \cdot 8H_2O$), 0.2614 g of $Co(OH)_2$ (or 0.0896 g of FeO), and 2 mL of 3.75 M H_3PO_4 for 60 h at 500 °C gave single-phase crystalline

* Abstract published in *Advance ACS Abstracts*, September 1, 1993.

(1) Lii, K. H.; Tsai, H. J.; Wang, S. L. *J. Solid State Chem.* **1990**, *87*, 396.
(2) Lii, K. H.; Li, C. H.; Cheng, C. Y.; Wang, S. L. *J. Solid State Chem.* **1991**, *95*, 352.
(3) Lii, K. H.; Chueh, B. R.; Kang, H.Y.; Wang, S. L. *J. Solid State Chem.* **1992**, *99*, 72.
(4) Wang, S. L.; Kang, H. Y.; Cheng, C. Y.; Lii, K. H. *Inorg. Chem.* **1991**, *30*, 3496.
(5) Lii, K. H.; Mao, L. F. *J. Solid State Chem.* **1992**, *96*, 436.
(6) Kang, H. Y.; Lee, W. C.; Wang, S. L.; Lii, K. H. *Inorg. Chem.* **1992**, *31*, 4743.
(7) Lii, K. H.; Wen, N. S.; Su, C. C.; Chueh, B. R. *Inorg. Chem.* **1992**, *31*, 439.
(8) Moore, P. B. *Am. Mineral.* **1970**, *55*, 135.
(9) Lii, K. H.; Dong, T. Y.; Cheng, C. Y.; Wang, S. L. *J. Chem. Soc., Dalton Trans.* **1993**, 577.
(10) Lii, K. H. Unpublished research.
(11) Dvoncova, E.; Lii, K.-H. *Inorg. Chem.*, preceding paper in this issue.

0020-1669/93/1332-4373$04.00/0

products of purple $CaCo_3(P_2O_7)_2$ and pale green $SrFe_3(P_2O_7)_2$. The solid-state reaction of SrO, FeO, and P_2O_5 (molar ratio 1:3:2) at 900 °C for 2 d also led to a single-phase of $SrFe_3(P_2O_7)_2$. The Co compound has not been produced in the form of a single phase by a solid-state reaction.

In addition, shown by X-ray powder analysis, the following isostructural compounds have been prepared have hydrothermal reactions: $AM_3(P_2O_7)_2$ (A = Sr, Ba; M = Ni, Co) and $BaFe_3(P_2O_7)_2$. All of them are stable in air. The Mg compounds and $CaFe_3(P_2O_7)_2$ have not been obtained. Crystals for X-ray structure analysis were obtained from hydrothermal reactions. The sample of $SrFe_3(P_2O_7)_2$ used for magnetic susceptbility and Mossbauer spectroscopy studies was prepared from a solid-state reaction. Solid-state reactions yielded polycrystalline products only.

Single-Crystal X-ray Diffraction. Three crystals having dimensions of 0.12 × 0.11 × 0.05 mm for $CaNi_3(P_2O_7)_2$, 0.10 × 0.05 × 0.03 mm for $CaCo_3(P_2O_7)_2$, and 0.30 × 0.30 × 0.10 mm for $SrFe_3(P_2O_7)_2$ were selected for indexing and intensity data collection on a Nicolet R3m/V four-circle diffractometer (for the Ni compound) and an Enraf-Nonius CAD4 diffractometer with κ-axis geometry (for the Co and Fe compounds) using monochromated Mo Kα radiation. Axial oscillation photographs along the three axes were taken to check the symmetry properties and unit cell parameters. Octants collected: $CaNi_3(P_2O_7)_2$, $+h,+k,\pm l$; $CaCo_3(P_2O_7)_2$, $\pm h,+k,+l$; $SrFe_3(P_2O_7)_2$, $\pm h,+k,+l$. The intensity data for all three crystals were corrected for Lorentz–polarization and absorption effects. Correction for absorption effects were based on ψ sans of a few suitable reflections with χ values close to 90° using the NRC VAX program package[12] (for the Co and Fe compounds) and the program XEMP of the SHELXTL-PLUS program package[13] (for the Ni compound). On the basis of systematic absences and successful solution and refinement of the structures, the space groups were determined to be $P2_1/c$ for all three compounds. Direct methods were used to locate the metal atoms with the other atoms being found from successive difference maps. All three structures were refined by full-matrix least-squares procedures based on F values. All atoms were refined with anisotropic temperature factors. The multiplicities of the alkaline-earth metal atoms were allowed to vary but did not deviate significantly from full occupancy. Corrections for anomalous dispersion for all three compounds and secondary extinction for $SrFe_3(P_2O_7)_2$ were made. Neutral-atom scattering factors were used.[14] Structure determination and refinement were performed on DEC Micro VAX computer systems using the SHELXTL-PLUS program packages.[13]

Magnetic Susceptibility and Mossbauer Spectroscopy. Magnetization data were obtained on polycrystalline $SrFe_3(P_2O_7)_2$ from 2 to 300 K in a magnetic field of 5 kG after zero-field cooling using a SQUID magnetometer. Observed susceptibilities were corrected for diamagnetism according to Selwood.[15]

The ^{57}Fe Mossbauer spectra of $SrFe_3(P_2O_7)_2$ were recorded at 300 and 77 K on a constant acceleration type instrument as reported elsewhere.[16] Velocity calibrations were made using a 99.99% pure 10-μm iron foil. Typical line widths for all three pairs of iron lines fell in the range 0.28–0.30 mm/s. Isomer shifts are reported with respect to iron foil at 300 K. It should be noted that the isomer shifts illustrated are plotted as experimentally obtained.

Results and Discussion

Structure. The crystallographic data for $CaNi_3(P_2O_7)_2$, $CaCo_3(P_2O_7)_2$, and $SrFe_3(P_2O_7)_2$ are listed in Table I, atomic coordinates and thermal parameters in Table II, and selected bond distances and bond valence sums[17] in Table III. Bond valence sums for the calcium metal ions are significantly smaller than +2. The coordination number of each alkaline-earth metal was determined on the basis of the maximum gap in the A–O distances ranked in increasing order. Each A^{2+} cation is coordinated by eight oxygen atoms; the ninth A–O distance is longer than 3.3 Å. Bond valence sums for other cations are in good accordance with their formal oxidation states. The alkaline-earth metals and M(2) sit on inversion centers, and all other atoms are at general positions. In the following, only the structure of $CaNi_3(P_2O_7)_2$ will be discussed because the three compounds are isostructural.

In $CaNi_3(P_2O_7)_2$ the NiO_6 octahedra are distorted and the octahedral distortion can be estimated by using the equation $\Delta = (1/6)\sum((R_i - \bar{R})/\bar{R})^2$, where R_i = an individual bond length

Table I. Crystallographic Data for $CaNi_3(P_2O_7)_2$ (I), $CaCo_3(P_2O_7)_2$ (II), and $SrFe_3(Pr_2O_7)_2$ (III)

	I	II	III
empirical formula	$CaNi_3O_{14}P_4$	$CaCo_3O_{14}P_4$	$Fe_3O_{14}P_4Sr$
color	yellow	purple	pale green
fw	564.09	564.76	603.04
space group	$P2_1/c$	$P2_1/c$	$P2_1/c$
a, Å	7.330(3)	7.394(1)	7.553(1)
b, Å	7.589(3)	7.6266(9)	7.7477(8)
c, Å	9.400(3)	9.444(2)	9.5796(8)
β, deg	111.90(3)	111.73(2)	112.11(1)
V, Å^3	485.1(3)	494.7(1)	519.4(1)
Z	2	2	2
T, °C	24	23	23
λ, Å	0.710 73	0.709 30	0.709 30
ρ_{calcd}, g/cm^3	3.861	3.791	3.856
μ, cm^{-1}	70.5	623	99.2
max 2θ, deg	55	55	55
$R(F_o)^a$	0.026	0.035	0.029
$R_w(F_o)^b$	0.037	0.037	0.032

^{a} $R = \sum||F_o| - |F_c||/\sum|F_o|$. ^{b} $R_w = \sum w(|F_o| - |F_c|)^2/\sum w|F_o|^2$, $w = [\sigma(F)^2 + gF^2]^{-1}$.

Table II. Positional Parameters and Thermal Parameters (Å^2 × 100) for $CaNi_3(P_2O_7)_2$ (I), $CaCo_3(P_2O_7)_2$ (II), and $SrFe_3(P_2O_7)_2$ (III)

	x	y	z	U_{eq}[a]
		Compound I		
Ca	0.5	0	0	1.01(3)
Ni(1)	0.18474(7)	0.62706(6)	0.02500(5)	0.69(2)
Ni(2)	0	0	0	0.58(2)
P(1)	0.8802(1)	0.7044(1)	0.1915(1)	0.47(3)
P(2)	0.5977(1)	0.4335(1)	0.2032(1)	0.55(3)
O(1)	0.3921(4)	0.4730(4)	0.1948(3)	1.10(9)
O(2)	0.0104(4)	0.2122(3)	0.1360(3)	0.69(8)
O(3)	0.9718(4)	0.5766(3)	0.1126(3)	0.87(8)
O(4)	0.6726(4)	0.6226(3)	0.1745(3)	0.98(8)
O(5)	0.6213(4)	0.3059(3)	0.0877(3)	0.99(8)
O(6)	0.2715(4)	0.8807(3)	0.1311(3)	0.84(8)
O(7)	0.83144(4)	0.8781(3)	0.1069(3)	0.63(8)
		Compound II		
Ca(1)	0.5	0	0	1.31(6)
Co(1)	0.1873(1)	0.6260(1)	0.0274(1)	0.89(3)
Co(2)	0	0	0	0.82(4)
P(1)	0.8785(3)	0.7048(2)	0.1918(2)	0.69(5)
P(2)	0.5974(2)	0.4339(2)	0.2038(2)	0.78(5)
O(1)	0.3936(7)	0.4755(6)	0.1937(5)	1.2(2)
O(2)	0.0105(7)	0.2127(6)	0.1371(5)	1.0(2)
O(3)	0.9725(7)	0.5789(6)	0.1138(5)	1.0(2)
O(4)	0.6739(7)	0.6211(6)	0.1746(6)	1.1(2)
O(5)	0.6201(7)	0.3065(6)	0.0892(5)	1.3(2)
O(6)	0.2761(7)	0.8820(6)	0.1318(5)	1.0(2)
O(7)	0.8286(7)	0.8780(6)	0.1072(5)	0.9(2)
		Compound III		
Sr	0.5	0	0	1.05(2)
Fe(1)	0.18942(7)	0.62318(6)	0.02882(6)	0.81(2)
Fe(2)	0	0	0	0.77(3)
P(1)	0.8868(1)	0.7045(1)	0.19313(9)	0.69(3)
P(2)	0.6030(1)	0.4447(1)	0.2032(1)	0.70(3)
O(1)	0.4030(4)	0.4876(3)	0.1954(3)	1.04(9)
O(2)	0.0003(4)	0.2159(3)	0.1381(3)	1.12(8)
O(3)	0.9717(3)	0.5772(3)	0.1140(3)	1.02(8)
O(4)	0.6834(4)	0.6287(3)	0.1792(3)	0.97(8)
O(5)	0.6180(3)	0.3198(3)	0.0869(3)	1.01(8)
O(6)	0.2747(4)	0.8873(3)	0.1356(3)	0.99(8)
O(7)	0.8420(4)	0.8746(3)	0.1096(3)	0.99(8)

[a] U_{eq} is defined as one-third of the trace of the orthtongalized U_{ij} tensor.

(12) Gabe, E. J.; Le Page, Y.; Charland, J. P.; Lee, F. L. *J. Appl. Crystallogr.* **1989**, *22*, 384.
(13) Sheldrick, G. M. *SHELXTL-PLUS Crystallographic System, Release 4.11*; Siemens Analytical X-Ray Instruments, Inc.: Madison, WI, 1990.
(14) *International Tables for X-Ray Crystallography*; Kynoch Press: Birmingham, England, 1974; Vol. IV.
(15) Selwood, P. W. *Magnetochemistry*; Interscience: New York, 1956.
(16) Dong, T. Y.; Schei, C. C.; Hsu, T. L.; Lee, S. L.; Li, S. J. *Inorg. Chem.* **1991**, *30*, 2457.
(17) Brown, I. D.; Altermatt, D. *Acta Crystallogr.* **1985**, *B41*, 244.

Table III. Selected Bond Lengths (Å) and Bond Valence Sunms ($\sum s$) for $CaNi_3(P_2O_7)_2$ (I), $CaCo_3(P_2O_7)_2$ (II), and $SrFe_3(P_2O_7)_2$ (III)

	Compound I		
Ca–O(1)	2.684(3) (2×)	Ni(2)–O(2)	2.039(3) (2×)
Ca–O(5)	2.513(3) (2×)	Ni(2)–O(5)	2.114(3) (2×)
Ca–O(6)	2.586(3) (2×)	Ni(2)–O(7)	2.078(3) (2×)
Ca–O(7)	2.439(3) (2×)	$\sum s$(Ni(2)–O) = 1.92	
$\sum s$(Ca–O) = 168		P(1)–O(2)	1.519(2)
Ni(1)–O(1)	2.102(3)	P(1)–O(3)	1.521(3)
Ni(1)–O(2)	2.052(2)	P(1)–O(4)	1.595(3)
Ni(1)–O(3)	2.054(4)	P(1)–O(7)	1.512(3)
Ni(1)–O(3)	2.067(3)	$\sum s$(P(1)–O) = 4.99	
Ni(1)–O(5)	2.127(4)	P(2)–O(1)	1.509(3)
Ni(1)–O(6)	2.152(3)	P(2)–O(4)	1.595(3)
$\sum s$(Ni(1)–O) = 1.84		P(2)–O(5)	1.512(3)
Ni(1)···Ni(1)	3.213(2)	P(2)–O(6)	1.547(2)
Ni(1)···Ni(2)	3.108(1)	$\sum s$(P(2)–O) = 4.94	
	Compound II		
Ca–O(1)	2.709(5) (2×)	Co(2)–O(2)	2.059(5) (2×)
Ca–O(5)	2.531(5) (2×)	Co(2)–O(6)	2.155(4) (2×)
Ca–O(6)	2.574(5) (2×)	Co(2)–O(7)	2.109(6) (2×)
Ca–O(7)	2.444(5) (2×)	$\sum s$(Co(2)–O) 1.96	
$\sum s$(Ca–O) = 1.65		P(1)–O(2)	1.518(5)
Co(1)–O(1)	2.083(4)	P(1)–O(3)	1.526(6)
Co(1)–O(2)	2.094(4)	P(1)–O(4)	1.594(6)
Co(1)–O(3)	2.068(6)	P(1)–O(7)	1.517(5)
Co(1)–O(3)	2.110(4)	$\sum s$(P(1)–O) = 4.95	
Co(1)–O(5)	2.161(6)	P(2)–O(1)	1.508(6)
Co(1)–O(6)	2.175(5)	P(2)–O(4)	1.597(5)
$\sum s$(Co(1)–O) = 1.92		P(2)–O(5)	1.509(6)
Co(1)···Co(1)	3.252(2)	P(2)–O(6)	1.539(4)
Co(1)···Co(2)	3.139(1)	$\sum s$(P(2)–O) = 4.98	
	Compound III		
Sr–O(1)	2.730(3) (2×)	Fe(2)–O(2)	2.132(2) (2×)
Sr–O(5)	2.659(2) (2×)	Fe(2)–O(6)	2.174(2) (2×)
Sr–O(6)	2.648(3) (2×)	Fe(2)–O(7)	2.101(3) (2×)
Sr–O(7)	2.584(2) (2×)	$\sum s$(Fe(2)–O) = 2.03	
$\sum s$(Sr–O) = 1.89		P(1)–O(2)	1.520(2)
Fe(1)–O(1)	2.077(2)	P(1)–O(3)	1.525(3)
Fe(1)–O(2)	2.107(2)	P(1)–O(4)	1.603(3)
Fe(1)–O(3)	2.123(3)	P(1)–O(7)	1.513(2)
Fe(1)–O(3)	2.123(2)	$\sum s$(P(1)–O) = 4.95	
Fe(1)–O(5)	2.180(3)	P(2)–O(1)	1.521(3)
Fe(1)–O(6)	2.270(2)	P(2)–O(4)	1.600(3)
$\sum s$(Fe(1)–O) = 1.99		P(2)–O(5)	1.512(3)
Fe(1)···Fe(1)	3.308(1)	P(2)–O(6)	1.537(2)
Fe(1)···Fe(2)	3.217(1)	$\sum s$(P(2)–O) = 4.91	

and $\bar{R}$ = average bond length.[18] The calculation results indicate that the distortion in $Ni(1)O_6$ ($10^4\Delta = 3.28$) is more pronounced than that in $Ni(2)O_6$ ($10^4\Delta = 2.17$). The PO_4 tetrahedra of a P_2O_7 group are in a semieclipsed configuration. The P atoms are displaced away from the bridging oxygen atom, O(4), so that one longer and three shorter P–O bonds are formed. The P(1)–O(4)–P(2) bond angle is 135.3(2)°. A view of the $CaNi_3(P_2O_7)_2$ structure along the *b* axis appears in Figure 1. Infinite chains of NiO_6 octahedra are connected by P_2O_7 groups to form a three-dimensional architecture with channels parallel to the *b* axis. Calcium atoms are located in sites within the channels. As shown in Figure 2, each infinite chain consists of NiO_6 octahedra sharing either trans or skew edges. Atom Ni(1) is displaced from the centroid of the $Ni(1)O_6$ octahedron by 0.133 Å from its neighboring Ni atoms, indicative of the absence of nickel–nickel bonding. The Ni(1)···Ni(1) and Ni(1)···Ni(2) distances are 3.213 and 3.108 Å, respectively. The difference in octahedral distortion is probably caused by differences in the next-nearest neighborhood, i.e. cation–cation repulsion. Atom Ni(2) sits on an inversion center and has a more symmetric neighborhood. Each $Ni(1)O_6$ octahedron shares skew edges with one $Ni(1)O_6$ and one $Ni(2)O_6$, and each $Ni(2)O_6$ octahedron shares trans edges with two $Ni(1)O_6$. Oxygen atoms O(2), O(3), O(6) are shared by Ni atoms. Figure 3 is the Schlegel diagram[19] of the coordination

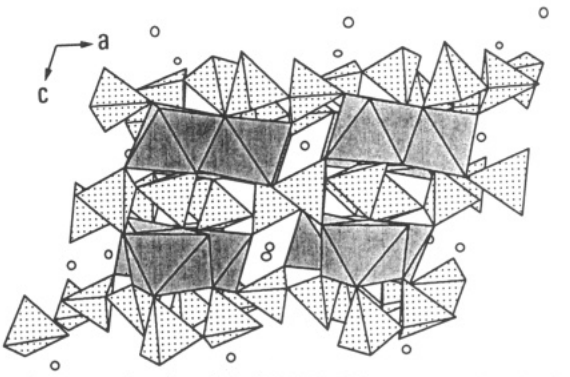

Figure 1. Perspective view of the $CaNi_3(P_2O_7)_2$ structure along the [010] direction. In this representation the corners of octahedra and tetrahedra are O atoms and the Ni and P atoms are at the center of each octahedron and tetrahedron, respectively. The open circles are Ca atoms.

polyhedra of the Ni atoms showing how the next-nearest neighbors are arranged in the structure. The lengths of the common edges are 2.581 and 2.683 Å and are considerably shorter than those of edges which are not shared. The shortening of shared edges is evidence that the structure is predominantly ionic. Each P_2O_7 group shares its six O atom vertices with five $Ni(1)O_6$ and two $Ni(2)O_6$ octahedra, which belong to three different infinite chains (Figure 4). Oxygen atoms O(3), O(5), and O(7) of a diphosphate group are coordinated to Ni atoms within a chain. Atoms O(1), O(2), and O(6) are coordinated to Ni atoms in two adjacent chains.

Table IV shows the calculation of the basicity of the structural unit $[Ni_3(P_2O_7)_2]$. A coordination number of 3 is assigned to each oxygen. The Lewis basicity of the structural unit is 0.25 valence unit (vu). The most stable structure will form when the Lewis acid strength of the cation most closely matches the Lewis base strength of the structural unit.[20,21] Examination of the Lewis acid strengths calculated by Brown[21] indicates that the values of Ca (0.274 vu) and Sr (0.233 vu) agree and consequently $AM_3(P_2O_7)_2$ (A = Ca, Sr, M = Ni, Co; A = Sr, M = Fe) are stable compounds. On the basis of the Lewis acidity of 0.195 vu for Ba, it is unexpected that $BaM_3(P_2O_7)_2$ (M = Fe, Ni, Co) are also stable. The value for Mg (0.334 vu) accounts for the fact that the $AM_3(P_2O_7)_2$ structure cannot have Mg as an interstitial cation. The apparent instability of $CaF_3(P_2O_7)_2$ may be explained if one includes cation radii in addition to the Lewis acidity and basicity in the argumentation. If the size of the channels along the *b* axis is controlled mainly by the size of the transition metal, then Fe^{2+} in this structure type expands the channel size to an extent which cannot accommodate Ca^{2+} anymore. This is also in accordance with the increase in cell dimensions when one moves from the Ni compound to the Co and Fe compounds. This argumentation also explains the unusual low bond valence sums for Ca^{2+} ions, which indicate tensional stress. The problem is less severe for the larger Sr^{2+} ion. This stress would probably become too high in a hypothetical $CaFe_3(P_2O_7)_2$ structure and therefore makes this compound unstable.

Magnetic Susceptibility and Mossbauer Effect Results. Figure 5 shows the magnetic susceptibility and inverse magnetic susceptibility of $SrFe_3(P_2O_7)_2$ plotted as a function of temperature. The data above 26 K were described very well by a Curie–Weiss equation: $\chi_M = C/(T - \Theta)$ where $C = 9.65$ cm^3·K/mol and $\Theta = 3.96$ K. From the relation $C = N\mu_{eff}^2/3k_B$ one obtains the effective magnetic moment μ_{eff} per metal atom = 5.07. These results indicate that $SrFe_3(P_2O_7)_2$ is paramagnetic between 26 and 300 K with an effective magnetic moment expected of a high-spin Fe(II) compound. Below 26 K the magnetic susceptibility rises sharply to a maximum at 6 K and then decreases just

(18) Shannon, R. D. *Acta Crystallogr.* **1976**, *A32*, 751.
(19) Hoppe, R.; Koehler, J. *Z. Kristallogr.* **1988**, *183*, 77.
(20) Hawthorne, F. C. *Z. Kristallogr.* **1992**, *201*, 183.
(21) Brown, I. D. *Acta Crystallogr.* **1992**, *B48*, 553.

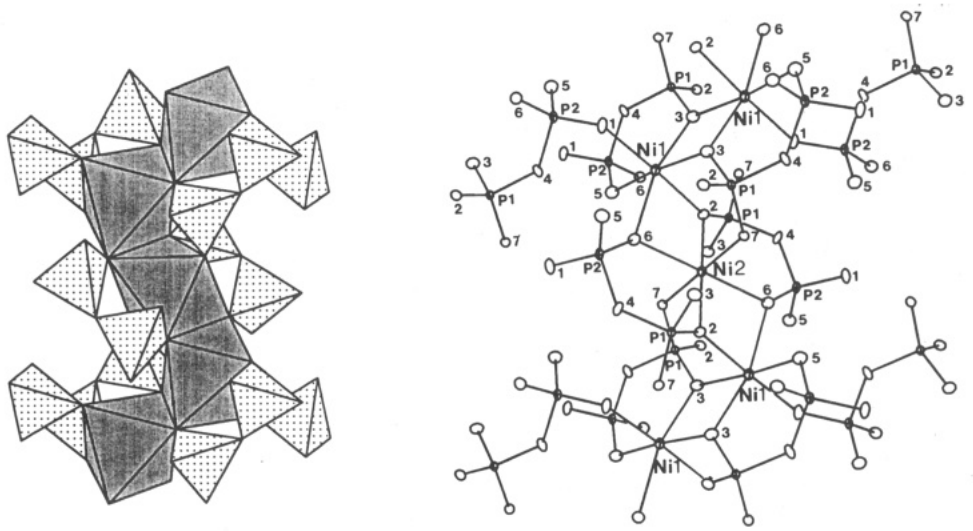

Figure 2. Left: Polyhedron representation of a section of an infinite chain in $CaNi_3(P_2O_7)_2$ as viewed along [001]. Right: ball-and-stick representation.

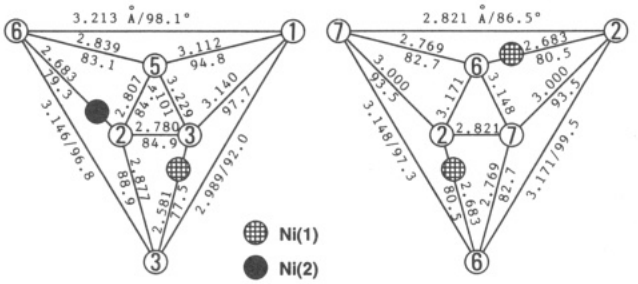

Figure 3. Left: Schlegel projection of a $Ni(1)O_6$ octahedron in $CaNi_3(P_2O_7)_2$. The central Ni atom is not shown in the projection. The O···O distances (Å) and their corresponding angles (deg) with respect to the central atom are indicated next to the edges. Right: Schlegel projection of a $Ni(2)O_6$ octahedron.

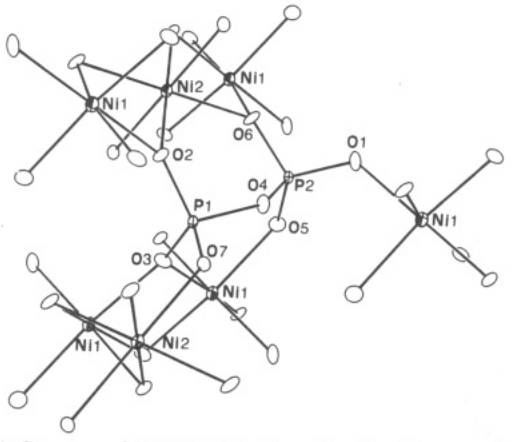

Figure 4. Structure of $CaNi_3(P_2O_7)_2$ viewed in a direction approximately parallel to [010], showing the connectivity of a P_2O_7 group to NiO_6 octahedra.

as sharply. This behavior could be due to unequal antiferromagnetic spin compensations of two nonequivalent Fe(II) ions. The maximum in the observed susceptibility at 6 K should correspond to the temperature of the maximum difference in magnetization of the two sublattices. However, we do not understand why Θ is not negative.

As shown in Figure 6, the room-temperature Mossbauer spectrum of $SrFe_3(P_2O_7)_2$ is a symmetric doublet and does not show two Fe components as expected from the crystal structure. A similar behavior was observed for the mineral neptunite.[22]

(22) Kunz, M.; Armbruster, T.; Lager, G. A.; Schultz, A. J.; Goyette, R. J.; Lottermoser, W.; Amthauer, G. *Phys. Chem. Miner.* **1991**, *18*, 199.

Table IV. Details of the Coordination of Different Anions in the Structural Unit of $CaNi_3(P_2O_7)_2$[a]

bonded atoms	no. of anions	ideal coordn no.	no. of bonds needed
P(1) + P(2)	$2\ ^{II}O(4)$	3	2
P + Ni	$2\ ^{II}O(1)$, $2\ ^{II}O(5)$, $2\ ^{II}O(7)$	3	6
P + 2 Ni	$2\ ^{III}O(2)$, $2\ ^{III}O(3)$, $2\ ^{III}O(6)$	3	0

[a] No. of bonded needed to structural unit = 6 + 2 = 8. Lewis basicity of structural unit = 2/8 = 0.25 vu.

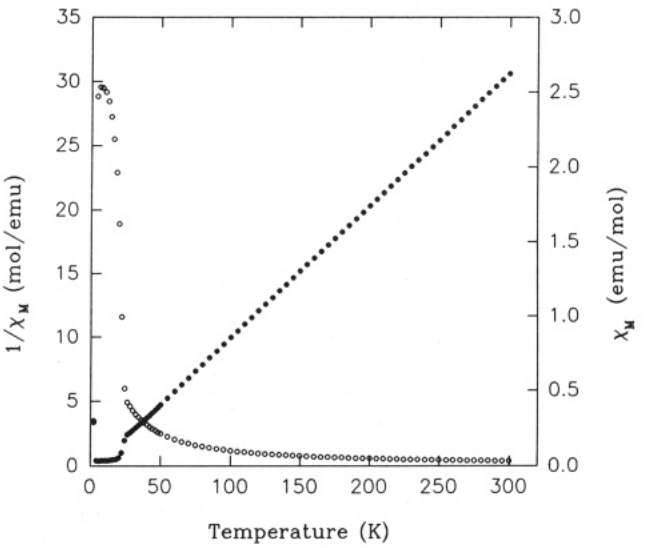

Figure 5. Magnetic susceptibility (χ_M, open circles) and inverse magnetic susceptibility ($1/\chi_M$, solid circles) plotted as a function of temperature for a powder sample of $SrFe_3(P_2O_7)_2$.

Although two distinct Fe positions were found in the structure of neptunite, 77 and 293 K spectra display only one quadrupole doublet. However, the two Fe sites can be resolved in the 400 K spectrum because the Fe environments become more different with rising temperature. Unfortunately, we are unable to record a high-temperature spectrum with our Mossbauer spectrometer. The spectrum of $SrFe_3(P_2O_7)_2$ was least-squares-fitted with one doublet. The obtained parameters are δ (isomer shift) = 1.28 mm/s, ΔE_Q (quadrupole splitting) = 3.14 mm/s, and Γ (full width at half-height) = 0.38 mm/s. The isomer shift is relative to iron at 300 K. The width for the line at more positive velocity is listed first. The line widths appear broader than those for a thin iron calibration foil. The large quadrupole splitting corresponds to large octahedral distortion. The isomer shift is

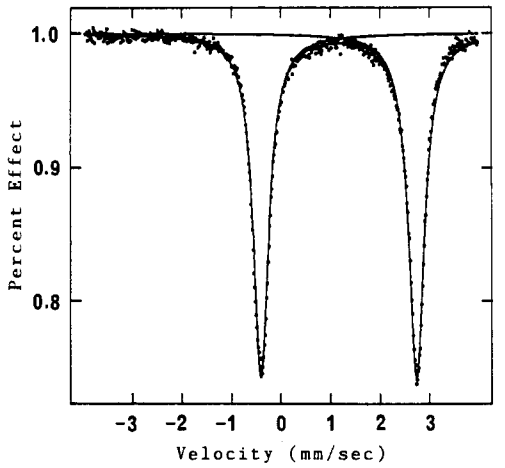

Figure 6. Mossbauer spectrum of $SrFe_3(P_2O_7)_2$ at 300 K.

characteristic of Fe(II). According to Menil,[23] the usual ranges of isomer shifts in oxides are 0.29–0.50 mm/s for Fe(III) in 6-coordination and 1.03–1.28 and 1.06–1.20 mm/s for Fe(II) in 6- and 5-coordinations, respectively. The very high value of the isomer shift for $SrFe_3(P_2O_7)_2$ indicates that the population of the 4s orbital is small and the Fe–O bond is highly ionic. The spectrum taken at 77 K displays a similar feature except that the low-temperature spectrum has a larger isomer shift and quadrupole splitting (δ = 1.39 mm/s, ΔE_Q = 3.25 mm/s). The Mossbauer studies on neptunite have also shown that quadrupole splitting and isomer shift decrease as the absorber temperature increases.[22]

Our efforts to grow crystals of transition-metal phosphates containing alkaline-earth metals by solid-state reactions have been unsuccessful, probably due to their very high melting points. Flux techniques could be used to prepare these crystals. The hydrothermal technique that we have used is useful for crystal growth of these phosphates, which are of interest because of their structural and magnetic properties. Further research on the hydrothermal synthesis of transition-metal phosphates is in progress.

Acknowledgment. Support for this study by the National Science Council and Institute of Chemistry, Academia Sinica of the Republic of China, is gratefully acknowledged. The authors thank Professor S.-L. Wang, Department of Chemistry, National Tsing Hua University, for the X-ray intensity data collection on $CaNi_3(P_2O_7)_2$, Professor T.-Y. Dong, Institute of Chemistry, Academia Sinica, for the Mossbauer spectroscopy measurements, and a reviewer for valuable comments.

Supplementary Material Available: Tables giving crystal data and details of the structure determinations, anisotropic thermal parameters, and bond lengths and angles (11 pages). Ordering information is given on any current masthead page.

(23) Menil, F. *J. Phys. Chem. Solids* **1985**, *46*, 763.